energyequipsys/ Vol 3/No2/Dec 2015/ 143-157

ENERGY QUIPSYS

Energy Equipment and Systems

http://energyequipsys.ut.ac.ir
www.energyeuquipsys.com

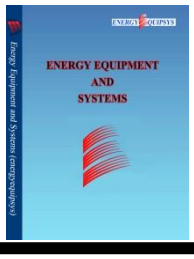

Active and reactive power control via currents of a rotor's *d* and *q* components with nonlinear predictive control strategy in a doubly fed induction generator based on wind power system

Authors

Hamed Javaheri Fard [a]
Hamid Reza Najafi [a*]
Hossein Eliasi [a]

[a] Faculty of Electrical and Computer Engineering, University of Birjand, Iran

Article history:

Received : 1 July 2015
Accepted : 28 October 2015

ABSTRACT

Wind energy today, has attracted widespread interest from among a variety of sources of renewable energy in the world. Owing to the increasing demand for production of electrical energy for electricity networks by using wind power, it is essential that wind power plants are actively incorporated in the network's performance using an appropriate control system. In general, these wind power plants consist of various types of wind turbines and generators, one of them being a doubly fed induction generator (DFIG). Strict and total control of DFIG is necessary for maintaining a high level of efficiency in utilizing the advantages and benefits of a modern wind plant. To achieve this aim, using the linear controllers is a difficult method because the wind plants involve some uncertainties. Nevertheless, there exists an unstable condition which may reduce the DFIG system's performance. In this research, a predictive control has been proposed for power control in order to overcome these problems. Control is established by optimizing a Cost Function considering the reality of the tracking factors. The prediction has been done on the basis of a DFIG model. Finally, results of the simulations carried out proved the performance of the controller.

Keywords: Active and Reactive Power Control, Doubly Fed Induction Generator, Model-Based Predictive Control, Wind Energy.

1. Introduction

Wind power is technologically and economically known to be a relatively steady source of electricity production [1]. Wind power systems account for being one of the important sources of renewable energy. Doubly fed induction generator (DFIG)-based systems have been widely used due to the low cost of convertors and the independent active and reactive power controls [2].

The DFIG stator can be directly connected to the grid, as also its rotor, by means of a two-sided convertor (Fig.1). The connection of the convertor to the rotor controls the active and reactive power between the DFIG stator and AC source, or an independent grid.

Vector control is one of the most common methods employed in the DFIG-based wind turbines [3]. A wind turbine control system is traditionally based on the orientation of the stator flux [4] and the orientation of the stator voltage [5]. This scheme divides the rotor current into active and reactive power components. The activ e and reactive power

*Corresponding author: Hamid Reza Najafi
Address: Faculty of Electrical and Computer Engineering, University of Birjand, Iran
E-mail address: h.r.najafi@birjand.ac.ir

control is obtained with a rotor current controller. Some researchers have used proportional-integral (PI) controllers and a vector control with stator flux orientation [6,7]. The problem of PI controllers, gains reformulation, and cross-coupling in DFIG is all in the implementation delimitation. There are interesting solutions written about these in references [8] and [9].

Research shows that using a predictive functional controller [10] and an internal controller [11] represents satisfactory performance when compared with a PI response. Utilization and implementation of this system is really difficult owing to the complex formulation of these two controllers. Another technique for power control of DFIG can be carried out with the aid of fuzzy logic [12]. These techniques can offer a relatively favorable power response, although the occurrence of errors in estimating the parameters can weaken the response.

Direct power control (DPC) is based on the principles of direct torque control [13]. DPC technique for DFIG control of power has been elaborated in reference [14]. This technique estimates the rotor voltage space vector based on the stator flux, and then accounts for power errors. In reference [15], DPC principles and implementation are obtained by hysteresis controllers and variable switching frequency. The basis of this method has been elaborated in references [16,17], and the simulation results have been presented using variables and constant switch frequencies, respectively. Moreover, the common DPC makes complex the design of AC filters due to its variable switch frequency. Power error vector control is an alternative for DPC [18]. This strategy has less complexity, and generates results similar to DPC.

Another method of control has been suggested for improving the performance of the controller [19]. This method reflects a proper performance although that is a demerit for this method of (power) control, in which the rotor's current, is increased by overshooting.

Predictive control is the method used in electrical machine drives [20] and inverters [21]. There is some research available on implementing this method in induction motor drives [22,23]. Operational predictive control has been established using a rotor current loop for DFIG power control [24] and predictive DPC established for DFIG [25]. This technique has a satisfactory power response, although control does not predict the outputs (active and reactive powers), and the power response may face reduction. In this case, a nonlinear model has been presented for DFIG predictive control which entails tedious and extra calculations [26].

In the second part of this paper, we have attempted to explain the model-based predictive control (MBPC). In the third part, modeling and dynamic performance of a DFIG has been presented. In the fourth and fifth parts, the control technique has been explained for stator flux orientation and implementation of machine rotor equations. The sixth part contains the implementation of a nonlinear predictive control strategy for DFIG. The seventh and final part gives the simulation results in order to observe the performance of the proposed controller.

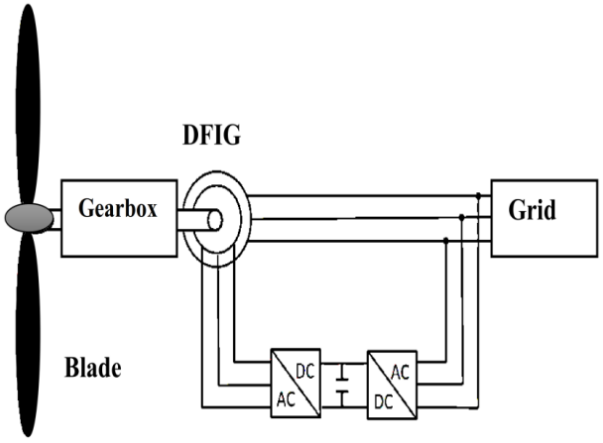

Fig.. 1. Configuration of a DFIG connected to a grid

Nomenclature

DFIG	Doubly fed induction generator
AC	Alternating current
PI	Proportional-integral
DPC	Direct power control
PID	Proportional-integral-derivative
Dq	Direct-axis & quadrature-axis
MBPC	Model-based predictive control
V_{ds}	Stator voltage in d reference-Volt
V_{qs}	Stator voltage in q reference-Volt
V_{dr}	Rotor voltage in d reference-Volt
V_{qr}	Rotor voltage in q reference-Volt
R_s	Stator resistance-Ω
R_r	Rotor resistance-Ω
L_{ls}	Stator inductance-Henry
L_{lr}	Rotor inductance-Henry
L_m	Mutual inductance-Henry
I_{ds}	Stator current in d reference-Amp
I_{qs}	Stator current in q reference-Amp
I_{dr}	Rotor current in d reference-Amp
I_{qr}	Rotor current in q reference-Amp
ω_e	Synchronous angular speed-Rad/sec
ω_r	Rotor's angular speed-Rad/sec
ϕ_{ds}	Stator flux in d reference-Weber
ϕ_{qs}	Stator flux in q reference-Weber
ϕ_{dr}	Rotor flux in d reference-Weber
ϕ_{qr}	Rotor flux in q reference-Weber
P_s	Stator's active power-Watt
Q_s	Stator's reactive power-Var
$\dot{\bar{X}}$	State variable derivative vector
$\bar{U}$	Input vector
$\bar{Y}$	Output vector
A	State matrix
B	Input matrix
C	Output matrix
I	Identity matrix
$\bar{X}(k+1)$	Discrete-time state equation
A_d	Discrete-time state matrix
B_d	Discrete input matrix
C_d	Discrete output matrix
T	Sampling period
k	Sampling time
m	First step of value of prediction of state variables
n_y	Predictive horizon
n_u	Control horizon
Z.M	Zero matrix
O	Number of outputs in Z.M
tra	Transpose
$\bar{X}_N(k)$	New state variable matrix
N	Letter indicates the new matrix
CF	Cost function
$w \in R^{(n_y \times q)\times 1}$	V Vector of future output references
$W_y \in R^{(n_y \times q)\times(n_y \times q)}$	A defined positive matrix
$W_u \in R^{n_u \times n_u}$	A defined positive matrix
q	Outputs

2. Model-based Predictive Control Strategy

MBPC being currently used in recent decades, has played a significant role in modern control engineering. This kind of control involves the widespread spectrum of applications, such as the chemical industry and even the food industry. The term, predictive control, does not denote a specific control method; it refers to the wide range of the control methods in which obtaining a control signal by using minimization of a Cost Function is possible through an explicit processing model. These design methods lead to the linear controllers which have the similar structure and the same degree of freedom. The basic idea which emerged in the predictive controls family is based on the following cases [27]:

- Using a model for predicting the output of the process in future times.
- Calculating a sequence control with the aid of minimizing of a Cost Function.
- Using the abandoning strategy which includes the utilization of the first control element in the calculated sequence control at any moment.

Different algorithms of MBPC among themselves are only different in the model used to display the process, noise and the Cost Function, which have to be minimized. This control method is widely used in the industry and in the academic sciences. Among the applications for this type of control are their uses in robot arms, steam generators, and so on. The good performance of these applications represents the potential of MBPC for obtaining the most effective control systems that can be used with any intervention over a long period of time.

In the following, some advantages of MBPC are presented [27]:

- This method can be easily implemented by having some knowledge about control, since the concepts are easy to be understood, and with relatively simple properties.
- This control method can be used for controlling an endless series of processes whether with simple dynamics or with complex dynamics including the systems with huge time delays, the phase nonminimum systems, or the unstable systems.

The multivariable systems can be easily controlled by means of this method.

- This method is suitable for the dead-time systems.

This method has its own disadvantages. First, deriving it (obtaining control signal) is more complex than that of the classic Proportional-Integral-Derivative (PID) controllers. If the dynamics of the process does not change, the controller coefficients can be predetermined, but all calculations must be repeated for each time sample in the case of adaptive control. While the constraints are taken into account, the extent of necessary calculations increases. Second, there is an urgent need for a proper model. However, the merits have superiority over demerits, making it very useful in the industry.

3. Modeling DFIG

The equivalent circuit of DFIG in *dq* reference frame is shown in Fig.2 [28].

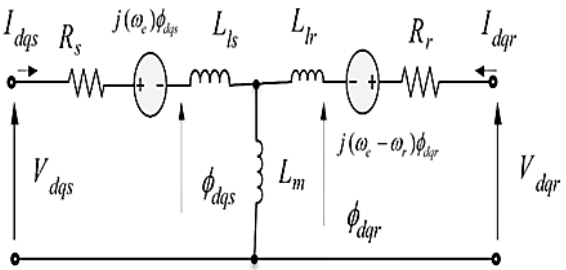

Fig. 2. DFIG equivalent circuit

Voltage and flux equations represent the behavior of DFIG in dq reference frame in the following relations [28]:

$$V_{ds} = R_s I_{ds} + \frac{d\phi_{ds}}{dt} - \omega_e \phi_{qs} \quad (1)$$

$$V_{qs} = R_s I_{qs} + \frac{d\phi_{qs}}{dt} + \omega_e \phi_{ds} \quad (2)$$

$$V_{dr} = R_r I_{dr} + \frac{d\phi_{dr}}{dt} - (\omega_e - \omega_r)\phi_{qr} \quad (3)$$

$$V_{qr} = R_r I_{qr} + \frac{d\phi_{qr}}{dt} + (\omega_e - \omega_r)\phi_{dr} \quad (4)$$

$$\phi_{ds} = L_{ls} I_{ds} + L_m (I_{ds} + I_{dr}) \quad (5)$$

$$\phi_{qs} = L_{ls} I_{qs} + L_m (I_{qs} + I_{qr}) \quad (6)$$

$$\phi_{dr} = L_{lr} I_{dr} + L_m (I_{ds} + I_{dr}) \quad (7)$$

and

$$\phi_{qr} = L_{lr} I_{qr} + L_m (I_{qs} + I_{qr}) \quad (8)$$

Equations 1, 2, 3 and 4, respectively, suggest the stator voltage in *d* reference, the stator voltage in *q* reference, the rotor voltage in *d* reference, and the rotor voltage in *q* reference. The relations 5, 6, 7 and 8, respectively, suggest the stator flux in *d* reference, the stator flux in *q* reference, the rotor flux in *d* reference, and the rotor flux in *q* reference. R_s, stator resistance; R_r, rotor resistance; I_{ds}, stator current in *d* reference; I_{qs}, stator current in *q* reference; I_{dr}, rotor current in d reference; I_{qr}, rotor current in *q* reference; ω_e, synchronous angular speed; ω_r, rotor's angular speed.

The stator's active and reactive powers are obtained from

$$P_s = \frac{3}{2}(V_{ds} I_{ds} + V_{qs} I_{qs}) \quad (9)$$

and

$$Q_s = \frac{3}{2}(V_{qs} I_{ds} - V_{ds} I_{qs}) \quad (10)$$

4. Control Method by Stator Flux Orientation

With respect to Fig.3, in the method control by stator flux orientation, the stator flux is placed on the *d* axis. This method is to detach the *d* and *q* axes so that all stator flux is oriented on the *d* axis, thus,

$$\phi_s = \phi_{ds} = L_{ls} I_{ds} + L_m (I_{ds} + I_{dr}), \quad \phi_{qs} = 0 \quad (11)$$

Moreover, all stator flux is oriented on the *q* axis, thus,

$$V_s = V_{qs} = R_s I_{qs} + \frac{d\phi_{qs}}{dt} + \omega_e \phi_{ds}, \quad V_{ds} = 0 \quad (12)$$

Therefore, using this principle, the stator's currents in longitudinal and transverse components, according to Eqs.5 and 6, are rewritten as

$$I_{ds} = \frac{1}{L_{ls} + L_m}(\phi_s - L_m (I_{dr})) \quad (13)$$

and

$$I_{qs} = -\frac{L_m}{L_{ls} + L_m}(I_{qr}) \quad (14)$$

Moreover, active and reactive powers in Eqs.9 and 10 are converted as

$$P_s = -\frac{3}{2} V_s \left(\frac{L_m}{L_{ls} + L_m}(I_{qr}) \right) \quad (15)$$

and

$$Q_s = \frac{3}{2} V_s \left(\frac{1}{L_{ls} + L_m}(\phi_s - L_m (I_{dr})) \right) \quad (16)$$

As shown in Eqs.13–16, the currents of the rotor are reflected both in the stator current and in the active and reactive power. Therefore, controlling power is possible by controlling the rotor's currents.

5. Rotor Side Equations

With Eqs.7 and 8, and putting them in Eqs.3 and 4, namely, the rotor's voltage in the transverse and longitudinal axis components, V_{dr} and V_{qr} are rewritten. This rewriting will be used in state equations of rotor's currents of transverse and longitudinal axis components, I_{dr} and I_{qr}. Therefore,

$$V_{dr} = R_r I_{dr} + L_{lr} \frac{dI_{dr}}{dt} + L_m \frac{dI_{ds}}{dt} + L_m \frac{dI_{dr}}{dt} - \omega_e L_{lr} I_{qr} - \omega_e L_m I_{qs} - \omega_e L_m I_{qr} + \omega_r L_{lr} I_{qr} + \omega_r L_m I_{qs} + \omega_r L_m I_{qr}$$

$$V_{qr} = R_r I_{qr} + L_{lr} \frac{dI_{qr}}{dt} + L_m \frac{dI_{qs}}{dt} + L_m \frac{dI_{qr}}{dt} + \omega_e L_{lr} I_{dr} + \omega_e L_m I_{ds} + \omega_e L_m I_{dr} - \omega_r L_{lr} I_{dr} - \omega_r L_m I_{ds} - \omega_r L_m I_{dr}$$

The above equations are rearranged as

$$V_{dr} = L_m \frac{d}{dt} I_{ds} + \left(-L_m (\omega_e - \omega_r)\right) I_{qs} + \left(R_r + (L_{lr} + L_m) \frac{d}{dt} \right) I_{dr} - (\omega_e - \omega_r)(L_{lr} + L_m) I_{qr} \quad (17)$$

and

$$V_{qr} = L_m (\omega_e - \omega_r) I_{ds} + \left(L_m \frac{d}{dt} \right) I_{qs} + \left(R_r + (L_{lr} + L_m) \frac{d}{dt} \right) I_{dr} + (\omega_e - \omega_r)(L_{lr} + L_m) I_{qr} \quad (18)$$

Putting Eqs.13 and 14 in 17 and 18, the state equation of rotor currents and DFIG model are obtained using

$$a' = \frac{R_r}{\Upsilon L_m - L_m - L_{lr}} \qquad b' = (\omega_e - \omega_r)$$

$$c' = -(\omega_e - \omega_r) + \frac{1}{\Upsilon L_m} \left(R_r + (L_m + L_{lr}) \left(\frac{R_r}{\Upsilon L_m - L_m - L_{lr}} \right) \right)$$

$$d' = \frac{2}{\Upsilon L_m} (\omega_e - \omega_r)(L_m + L_{lr}) \quad (19)$$

$$\begin{bmatrix} \frac{dI_{dr}}{dt} \\ \frac{dI_{qr}}{dt} \end{bmatrix} = \begin{pmatrix} a' & b' \\ c' & d' \end{pmatrix} \begin{bmatrix} I_{dr} \\ I_{qr} \end{bmatrix} + \begin{pmatrix} \frac{-1}{\Upsilon L_m - L_m - L_{lr}} & 0 \\ \frac{-1}{\Upsilon L_m (\Upsilon L_m - L_m - L_{lr})} (L_m + L_{lr}) & \frac{-1}{\Upsilon L_m} \end{pmatrix} \begin{bmatrix} V_{dr} \\ V_{qr} \end{bmatrix} + \begin{pmatrix} 1 & 0 \\ 0 & 1 \end{pmatrix} \begin{bmatrix} 0 \\ \frac{(\omega_e - \omega_r)}{L_m} \phi_s \end{bmatrix}$$

Equation 19 is presented as a state space equation. That is

$$\dot{\overline{X}} = A\overline{X} + B\overline{U}$$

$$\overline{Y} = C\overline{X}$$

And in Eq.19,

$$\Upsilon = \frac{L_m}{L_m + L_{ls}}$$

where the output matrix is an identity matrix

$$\mathrm{C} = I = \begin{pmatrix} 1 & 0 \\ 0 & 1 \end{pmatrix}.$$

6. Nonlinear Predictive Control Strategy for DFIG

Here, in order to design a predictive control for DFIG, Eq.19 is discretized as follows [29]:

$$\overline{\mathrm{X}}(k+1) = A_d \cdot \overline{\mathrm{X}}(k) + B_d \cdot \overline{\mathrm{U}}(k) \tag{20}$$

$$\overline{\mathrm{Y}}(k) = C_d \cdot \overline{\mathrm{X}}(k) \tag{21}$$

$$A_d = e^{AT} \cong I + \mathrm{A}T$$

$$B_d = \int_0^{\tau} e^{AT} B d\tau \cong \mathrm{B}T$$

$$C_d = \mathrm{C}$$

Equation 20 is rewritten as 22 by replacing the sampling times in both sides:

$$\overline{\mathrm{X}}(k+1) - \overline{\mathrm{X}}(k) = A_d\left(\overline{\mathrm{X}}(k) - \overline{\mathrm{X}}(k-1)\right) + B_d\left(\overline{\mathrm{U}}(k) - \overline{\mathrm{U}}(k-1)\right) \tag{22}$$

In Eq.22, the variables in the left and right of the equation, and the control variables, are separated and marked as follows:

$$\Delta\overline{\mathrm{X}}(k+1) = \overline{\mathrm{X}}(k+1) - \overline{\mathrm{X}}(k)$$

$$\Delta\overline{\mathrm{X}}(k) = \overline{\mathrm{X}}(k) - \overline{\mathrm{X}}(k-1)$$

$$\Delta\overline{\mathrm{U}}(k) = \overline{\mathrm{U}}(k) - \overline{\mathrm{U}}(k-1)$$

Let $m=1,2,\ldots,n$, then Eq.22 is by means of above-mentioned formulas:

$$\overline{\mathrm{X}}(k+1) - \overline{\mathrm{X}}(k) = A_d\left(\overline{\mathrm{X}}(k) - \overline{\mathrm{X}}(k-1)\right) + B_d\left(\overline{\mathrm{U}}(k) - \overline{\mathrm{U}}(k-1)\right) \Leftrightarrow$$

$$\overline{\mathrm{X}}(k+m) = \overline{\mathrm{X}}(k+m-1) + A_d\Delta\overline{\mathrm{X}}(k+m-1) + B_d\Delta\overline{\mathrm{U}}(k+m-1) \tag{23}$$

Equation 23 represents the first step of "m" value of prediction of state variables; "n_y" is the predictive horizon. Its selection is vital for performance of the control, since the selection of a high value for this parameter improves the stability of the system, but it can increase the values of calculations to more than what is needed.

Generally, the predictions in the length of predictive horizon and control horizon "n_u" are calculated as in the following equations:

$$\begin{aligned}
&\overline{\mathrm{X}}(k+1|k) = \overline{\mathrm{X}}(k) + A_d\Delta\overline{\mathrm{X}}(k) + B_d\Delta\overline{\mathrm{U}}(k) \rightarrow\rightarrow\rightarrow \\
&\overline{\mathrm{X}}(k+2|k) = \overline{\mathrm{X}}(k) + \left\{A_d + \left(A_d \times A_d\right)\right\}\Delta\overline{\mathrm{X}}(k) + \left(I + A_d\right)B_d\Delta\overline{\mathrm{U}}(k) + B_d\Delta\overline{\mathrm{U}}(k+1) \rightarrow\rightarrow\rightarrow \\
&\vdots \\
&\vdots
\end{aligned} \tag{24}$$

$$\overline{\mathrm{X}}(k+n_u-1|k) = \overline{\mathrm{X}}(k) + \left\{\sum_{b=1}^{n_u-1} A_d^b\right\}\Delta\overline{\mathrm{X}}(k) + \left\{\sum_{b=1}^{n_u} A_d^{b-1}\right\}B_d\Delta\overline{\mathrm{U}}(k) + \cdots\cdots + B_d\Delta\overline{\mathrm{U}}(k+n_u-2) \tag{25}$$

In control law, let n_u =1, then the input range is an average value that allows the outputs to comply with the reference values. Let n_u >1, then strategy control produces the control signals which cause the output to follow the reference closely and accurately. Selecting the large values for n_u, produces the large number of control signals and increases the values of calculations to more than what is needed.

If constructing the following matrices

$$X = \begin{bmatrix} \overline{\mathrm{X}}(k) \\ \overline{\mathrm{X}}(k+1|k) \\ \overline{\mathrm{X}}(k+2|k) \\ \overline{\mathrm{X}}(k+n_u-1|k) \end{bmatrix}$$

$$\Delta U = \begin{bmatrix} \Delta\overline{\mathrm{U}}(k) \\ \Delta\overline{\mathrm{U}}(k+1|k) \\ \Delta\overline{\mathrm{U}}(k+2|k) \\ \Delta\overline{\mathrm{U}}(k+n_u-1|k) \end{bmatrix}$$

then,

$$X = \mathrm{A}' \cdot \Delta U + \sigma \tag{26}$$

In Eq.26,

$$\mathrm{A}' = \begin{pmatrix} 0 & 0 & \cdots & 0 \\ B_d & 0 & \cdots & 0 \\ \vdots & \vdots & \vdots & \vdots \\ \left\{\sum_{b=1}^{n_u-1} A_d^{b-1}\right\}B_d & \left\{\sum_{b=1}^{n_u-2} A_d^{b-1}\right\}B_d & \cdots & 0 \end{pmatrix}$$

Also, in Eq.26, we have

$$\sigma = \begin{pmatrix} \bar{X}(k) \\ \bar{X}(k) + A_d \Delta\bar{X}(k) \\ \bar{X}(k) + \left\{ \sum_{b=1}^{2} A_d^b \right\} \Delta\bar{X}(k) \\ \vdots \\ \bar{X}(k) + \left\{ \sum_{b=1}^{n_u - 1} A_d^b \right\} \Delta\bar{X}(k) \end{pmatrix}$$

To incorporate the $\Delta\bar{X}(k)$ to $\bar{Y}(k)$ output, we construct a matrix with new state variables; but before rewriting Eq.22 in the form of Eq.27. Then,

$$\Delta\bar{X}(k+1) = A_d \cdot \Delta\bar{X}(k) + B_d \cdot \Delta\bar{U}(k) \quad (27)$$

In Eq.27, the input of the state space model is $\Delta\bar{U}(k)$.

In the following, we construct the new state variable matrix:

$$\bar{X}^N(k) = \begin{pmatrix} \Delta\bar{X}(k)^{tra} \\ \bar{Y}(k) \end{pmatrix} \quad (28)$$

In Eq.28, "tra" symbol is the transposition of the matrix, and the letter "N" indicates the new matrix.

Therefore, accounting for Eq.27 and the following Eq.29, we reach a new state space model in Eq.30:

$$\bar{Y}(k+1) - \bar{Y}(k) = C_d \left\{ \bar{X}(k+1) - \bar{X}(k) \right\} = C_d \left\{ \Delta\bar{X}(k+1) \right\} = C_d \left\{ A_d \Delta\bar{X}(k) + B_d \Delta\bar{U}(k) \right\} \quad (29)$$

$$\begin{pmatrix} \Delta\bar{X}(k+1) \\ \bar{Y}(k+1) \end{pmatrix} = \begin{pmatrix} A_d & \text{Z.M} \\ C_d \cdot A_d & I \end{pmatrix} \begin{pmatrix} \Delta\bar{X}(k) \\ \bar{Y}(k) \end{pmatrix} + \begin{pmatrix} B_d \\ C_d \cdot B_d \end{pmatrix} \Delta\bar{U}(k)$$

$$\bar{Y}(k) = \begin{pmatrix} \text{Z.M} & I \end{pmatrix} \begin{pmatrix} \Delta\bar{X}(k) \\ \bar{Y}(k) \end{pmatrix} \quad (30)$$

In Eq.30, "Z.M" represents a zero matrix, that is $\begin{pmatrix} 0 & \dots & 0 \\ \vdots & \ddots & \vdots \\ 0 & \cdots & 0 \end{pmatrix}_{O \times O}$, with $O \times O$ dimensions), in which O is the number of outputs, and "I" is an identity matrix with $O \times O$ dimensions.

The state space model in Eq.30 can be rewritten like Eq.31. Therefore,

$$\bar{X}^N(k+1) = A^N \cdot \bar{X}^N(k) + B^N \cdot \Delta\bar{U}(k)$$

$$\bar{Y}(k) = C^N \cdot \begin{pmatrix} \Delta\bar{X}(k) \\ \bar{Y}(k) \end{pmatrix} \quad (31)$$

Basing on the state space model, state, input and output matrices in Eq.31, the follow-up outputs will be calculated consecutively.

Current plant information is represented by means of $\bar{X}^N(k)$, assuming that the new state variable matrix is accessible through measurement in the sampling time *k*.

Future control trajectory is as follows:

$$\Delta\bar{U}(k)$$
$$\Delta\bar{U}(k+1)$$
$$\vdots$$
$$\Delta\bar{U}(k+n_u-1)$$

Having $\bar{X}^N(k)$, future state variables are predicted for n_y number of samples.

Defining $\Delta\bar{U}(k+m) = 0 \qquad m = n_u, \dots, n_y$, the future state variables are:

$$\bar{X}^N(k+1|k)$$
$$\vdots$$
$$\bar{X}^N(k+r|k)$$
$$\vdots$$
$$\bar{X}^N(k+n_y|k)$$

where, $\bar{X}^N(k+r|k)$ is to be the predicted state variable in $k+r$ with present and certain information $\bar{X}^N(k)$.

Future state variables have been calculated consecutively using the equation shown below,

$$\bar{X}^N(k+1|k) =$$
$$A^N \cdot \bar{X}^N(k) + B^N \cdot \Delta\bar{U}(k) \rightarrow\rightarrow\rightarrow$$
$$\bar{X}^N(k+2|k) =$$
$$A^N \cdot \bar{X}^N(k+1|k) + B^N \cdot \Delta\bar{U}(k+1) =$$
$$\left(A^N \times A^N\right)\bar{X}^N(k) + \left(A^N \times B^N\right)\Delta\bar{U}(k) +$$
$$B^N \Delta\bar{U}(k+1) \rightarrow\rightarrow\rightarrow$$
$$\vdots$$
$$\vdots$$

$$\overline{X}^{N}(k+n_y \mid k)=\left(A^{N}\right)^{n_y}\overline{X}^{N}(k)+\left(A^{N}\right)^{n_y-1}B^{N}\Delta\overline{U}(k)+\left(A^{N}\right)^{n_y-2}B^{N}\Delta\overline{U}(k+1)+\cdots+\left(A^{N}\right)^{n_y-n_u}B^{N}\Delta\overline{U}(k+n_u-1) \quad (32)$$

Through Eq.(32) and the predicted state variables, the predicted output variables have been calculated as follows:

$$\begin{aligned}&\overline{Y}(k+1\mid k)=\\&C^{N}A^{N}\cdot\overline{X}^{N}(k)+C^{N}B^{N}\cdot\Delta\overline{U}(k)\rightarrow\rightarrow\rightarrow\\&\overline{Y}(k+2\mid k)=\\&C^{N}A^{N}\cdot\overline{X}^{N}(k+1\mid k)+C^{N}B^{N}\cdot\Delta\overline{U}(k+1)=\\&\left(C^{N}\times A^{N}\times A^{N}\right)\overline{X}^{N}(k)+\left(C^{N}\times A^{N}\times B^{N}\right)\Delta\overline{U}(k)\\&+\left(C^{N}\times B^{N}\right)\Delta\overline{U}(k+1)\rightarrow\rightarrow\rightarrow\\&\vdots\\&\vdots\\&\overline{Y}(k+n_y\mid k)=C^{N}\left(A^{N}\right)^{n_y}\overline{X}^{N}(k)+\\&C^{N}\left(A^{N}\right)^{n_y-1}B^{N}\Delta\overline{U}(k)+\\&C^{N}\left(A^{N}\right)^{n_y-2}B^{N}\Delta\overline{U}(k+1)+\\&\cdots+C^{N}\left(A^{N}\right)^{n_y-n_u}B^{N}\Delta\overline{U}(k+n_u-1)\end{aligned} \quad (33)\text{–}(34)$$

The predicted variables have been formulated through considering the current information of state variable $\overline{X}^{N}$, and shift the sampling times in the future instants of

$$\Delta\overline{U}(k+m) \qquad m=0,1,2,\ldots n_u-1$$

In the following, we define the output matrix; its dimensions have been given for a "multi-input/multi-output" system.

$$Y=\begin{bmatrix}\overline{Y}(k+1\mid k)\\ \overline{Y}(k+2\mid k)\\ \vdots\\ \overline{Y}(k+n_y\mid k)\end{bmatrix}_{2n_y\times 1}^{\mathrm{tra}}$$

Therefore, incorporating Eq.33 and 34 into one frame,

$$Y=\begin{pmatrix}C^{N}A^{N}\\ C^{N}\left(A^{N}\right)^{2}\\ \vdots\\ C^{N}\left(A^{N}\right)^{n_y}\end{pmatrix}\underbrace{\begin{pmatrix}\Delta\overline{X}(k)\\ \overline{Y}(k)\end{pmatrix}}_{\overline{X}^{N}(k)}+b''\underbrace{\left(\Delta\overline{U}(k)\quad\cdots\quad\Delta\overline{U}(k+n_u-1\mid k)\right)}_{\Delta U} \quad (35)$$

$$b''=\begin{pmatrix}C^{N}B^{N} & 0 & 0 & \cdots & 0\\ C^{N}A^{N}B^{N} & C^{N}B^{N} & 0 & \cdots & 0\\ \vdots & & & & \\ \vdots & & & & \\ C^{N}\left(A^{N}\right)^{n_y-1}B^{N} & C^{N}\left(A^{N}\right)^{n_y-2}B^{N} & C^{N}\left(A^{N}\right)^{n_y-3}B^{N} & \cdots & C^{N}\left(A^{N}\right)^{n_y-n_u}B^{N}\end{pmatrix}$$

Or:

$$Y=E\cdot\overline{X}^{N}(k)+b''\cdot\Delta U \quad (36)$$

Cost Function, which is minimized at any sampling time, is a quadratic criterion:

$$CF=\left\{(Y-w)^{\mathrm{tra}}W_y(Y-w)\right\}+\left\{\Delta U^{\mathrm{tra}}W_u\Delta U\right\}$$
$$\Delta U_{\min}\le\Delta U\le\Delta U_{\max} \quad (37)$$

Where, $w\in R^{(n_y\times q)\times 1}$ indicates the vector of future output references in control state; $W_y\in R^{(n_y\times q)\times(n_y\times q)}$ represents a defined positive matrix which allows a confirmation of every controlled output and its predictions; $W_u\in R^{n_u\times n_u}$ indicates a defined positive matrix, usually diametric, which weighs the number of control efforts for inputs, and "q" stands for outputs.

7. Simulation Results

To begin simulation, we determine the DFIG parameters as shown in Table 1.

Table 1. Generator parameters

R_s	0.0234 Ω
R_r	0.0156 Ω
L_m	0.01678 H
L_{ls}	0.012587 H
L_{lr}	0.012587 H
V_s	580 V
N.P (pairs of poles)	2

The proposed strategy control has been simulated using Matlab/Simulink software.

Power control strategy has one time, $T=0.2\times10^{-4}$ (sec).

The following figures represent the experiments of the simulation.

The studies have been conducted based on the various steps of active and reactive power,

the rotor's constant speed of 222 radians per second, in order to test the dynamic response of proposed strategy for power control.

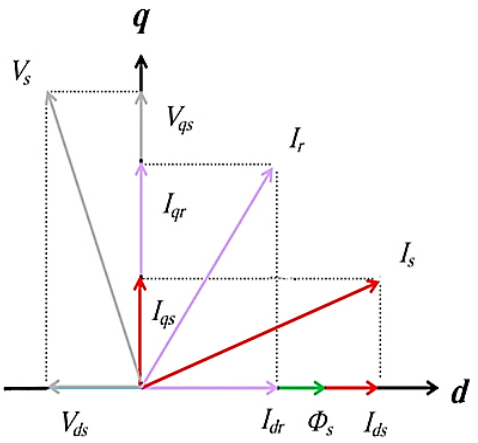

Fig. 3. Phasor diagram of control by stator flux orientation

In Fig.4, the dynamic performance of the proposed control strategy has been shown for steps of active and reactive power. As seen in the results of active and reactive power responses, it is to be said that the dynamic response for both powers are very fast. Initial reference for active power is −60 kw, and the power factor is 0.85. Then, the reference active power changes from −60 to −100, and power factor from 0.85 to −0.85 in 0.65 second. Again, the reference power changes from −100 to −149 kw; and the power factor from −0.85 to 1.0 in 0.9 second. In Fig.5, the *d* and *q* components have been shown. These responses also represent a good tracking performance. In Fig.6, three-phase stator currents, and in Fig.7, three-phase rotor currents have been depicted; these currents are sine. Overshoot is very small in the active and reactive power responses, in the three-phase stator currents, and in the three-phase rotor currents. Figure 8 represents the rotor speed as input in 222 radians per second in a constant manner. Figure 9 shows the DC link capacitor voltage as 415 V. The desirable performance of the control system is based on the fact that this system accords with the designed parameters. The control system certainly has good performance due to the compliance of powers with their own reference values.

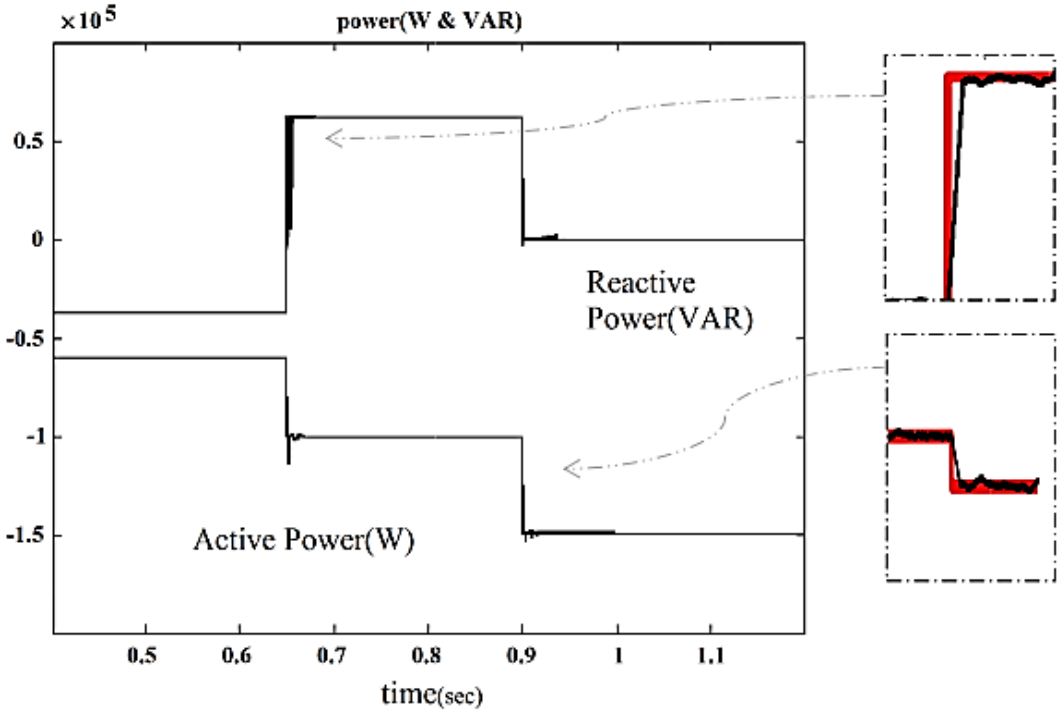

Fig. 4. Step test response for active and reactive power in a super-synchronous operation

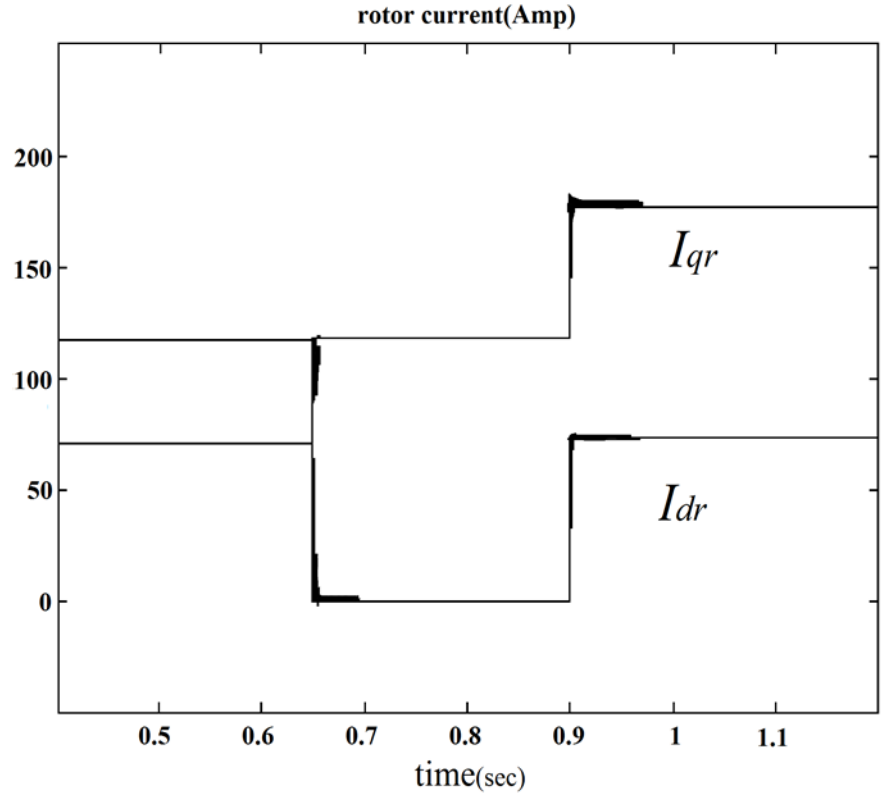

Fig. 5. Step test response for the rotor current's d & q axes in synchronous reference and a super-synchronous operation

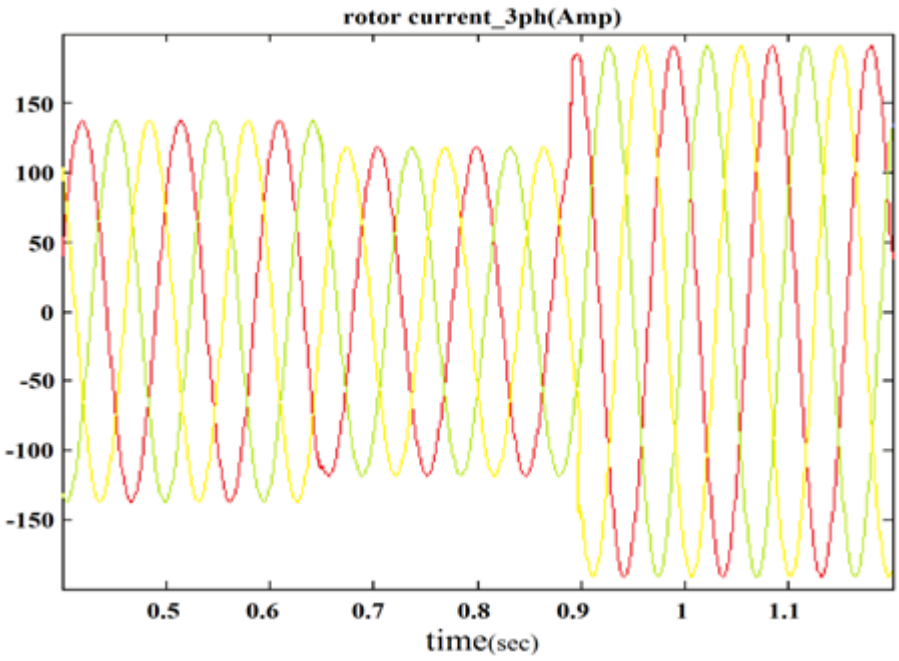

Fig. 6. Three-phase stator current in stationary reference

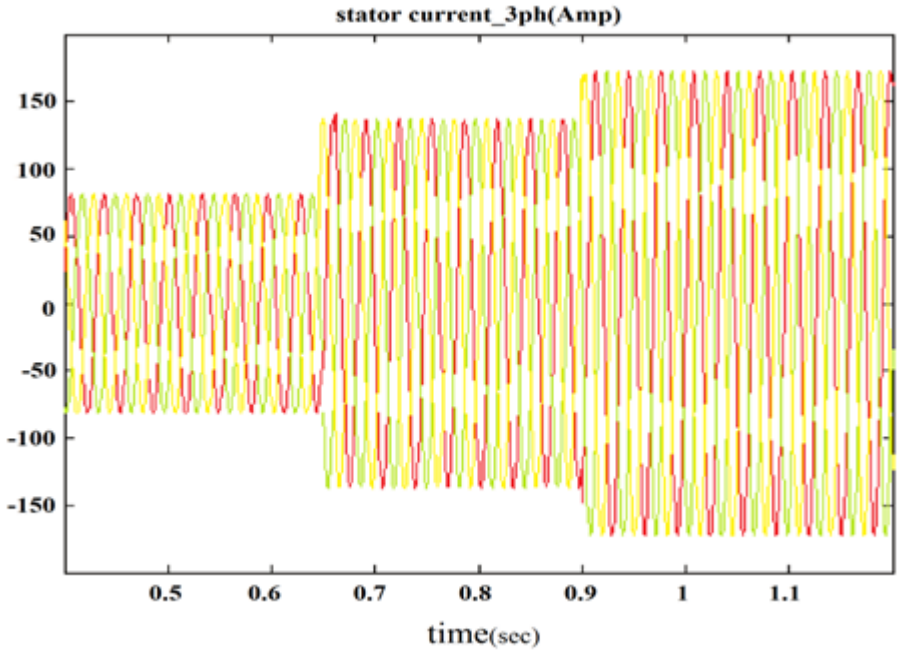

Fig. 7. Three-phase rotor current in stationary reference

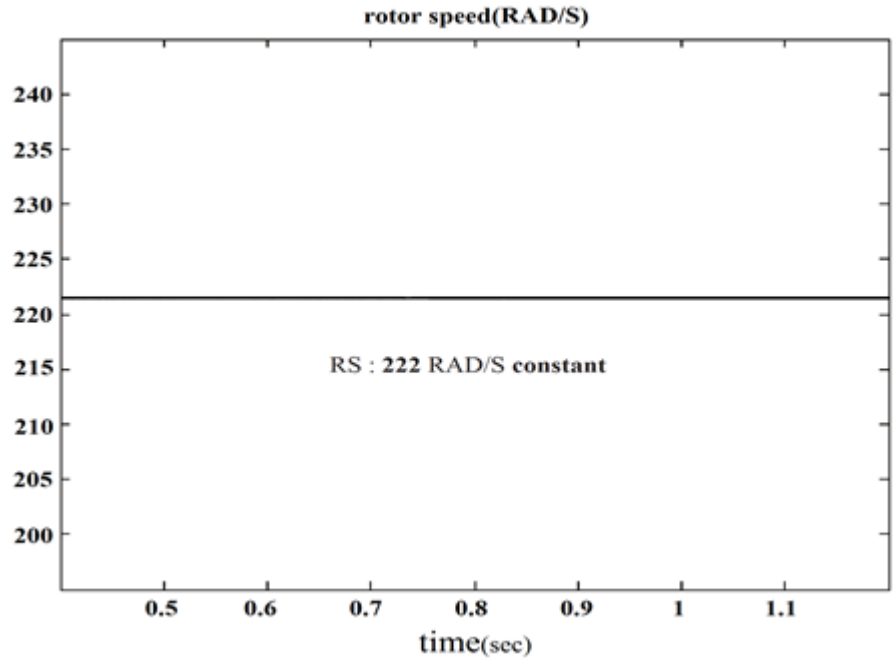

Fig. 8. Rotor speed as input (radian/sec) in stationary reference

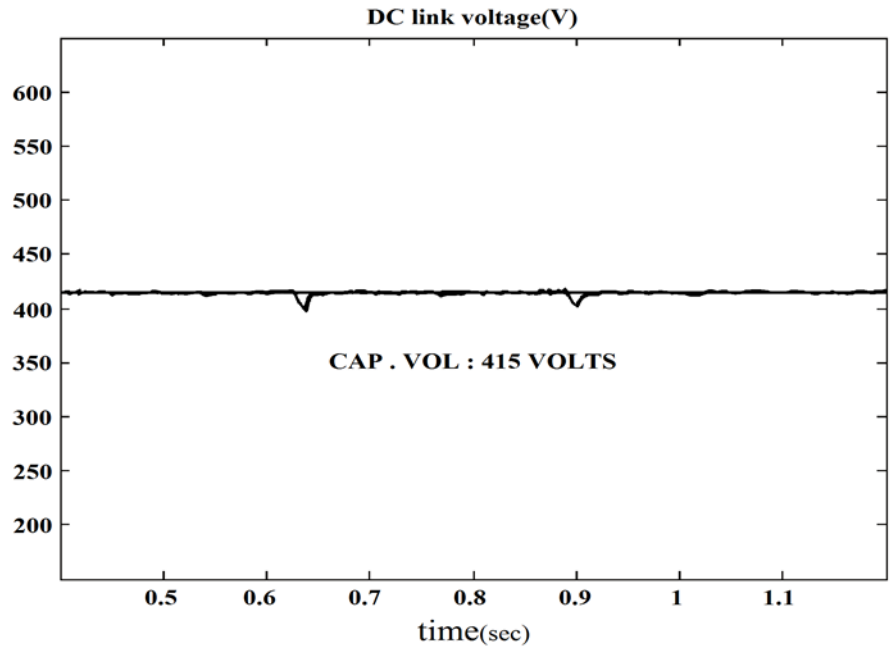

Fig. 9. DC link capacitor voltage between two converters in Fig.1

8. Conclusion

In this paper, an MBPC was presented in order to control the active and reactive powers of a wind turbine-based DFIG using *d* and *q* components. The MBPC is easily adaptable and executable for controlling the DFIG power. The predicted outputs have been calculated assisting a space-state model of DFIG. The control system has been composed of the control law which has been extracted by means of optimizing Cost Function which takes into account the control effort, the difference between predicted outputs (active and reactive powers), and the reference values. Rotor control voltage in the form of a receding horizon has been calculated while satisfying the state constraints. This control method applies the constant switching frequency which overcomes the problems of common and traditional 'direct power control', as found in reference [30]. The simulation results show the robustness and effectiveness of this control method. Future research may be conducted based on the implementation of a predictive control strategy in other renewable sources. For more information, refer to references [31–37], (previous works of the authors of this paper).

References

[1]Tourou P., Sourkounis C.: Review of Control Strategies for DFIG-Based Wind Turbines under Unsymmetrical Grid Faults, Ecological Vehicles and Renewable Energies (EVER), IEEE Conference Publications, (2014) 1-9.

[2]Boulâam K., Boukhelifa A.: A Fuzzy Sliding Mode Control for DFIG-Based Wind Turbine Power Maximisation, Power Electronics, Machines and Drives (PEMD), IET Conference Publications, (2014) 1-6.

[3]Mohammadi.J., Vaez-Zadeh S., Afsharnia S., Daryabeigi E.: A Combined Vector and Direct Power Control for DFIG-Based Wind Turbines, Sustainable Energy, IEEE Trans on, (2014) 767-775.

[4]Esmaeeli M.R., Kianinejad R., Razzaz M.: Field Oriented Control of DFIG Based on Modified MRAS Observer, Electrical Power Distribution Networks (EPDC), Proceedings of 17 th Conference on, (2012)1-7.

[5]Ozsoy E.E., Golubovic E., Sabanovic A. ,Gokasan M.,: A Stator Voltage Oriented Doubly Fed Induction Generator Control Method with a Disturbance Observer, EUROCON, IEEE, (2013)1102-1107.

[6]Shuhui Li., Challoo R., Nemmers M.J.,: Comparative Study of DFIG Power Control Using Stator-Voltage and Stator-Flux Oriented Frames, Power & Energy Society General Meeting, PES '09. IEEE, (2009)1- 8.

[7]Naguru N.R., Karthikeyan A., Nagamani C., Kumar V.S.,: Comparative Study of Power Control of DFIG Using PI Control and FeedBack Linearization Control,

Advances in Power Conversion and Energy Technologies (APCET), International Conference on, (2012)1-6.

[8] De Oliveira R. G., Da Silva J. L., Silva S. R., Development of a New Reactive power control strategy in doubly-fed induction generators for wind turbines, Eletrônica de Potência, (2008) Vol. 13, No. 4, 277-284.

[9] Poitiers F., Bouaouiche T., Machmoum M., Advanced Control of a Doubly-Fed Induction Generator for Wind Energy Conversion, Electric Power Syst. Res., (2009) Vol. 79, 1085-1096.

[10] Guolian H., Zhentao W., Pan J., Jianhua Z., Multivariable Predictive Functional Control Applied to Doubly Fed Induction Generator Under Unbalanced Grid Voltage Conditions, Industrial Electronics and Applications, ICIEA, 4th IEEE Conference on, (2009) 2644-2650.

[11] Guo J., Cai X., Gong Y., Decoupled Control of Active and Reactive Power for a Grid-Connected Doubly-Fed Induction Generator, in Proc. Third International Conference Electric Utility Deregulation and Restructuring and Power Technologies (DRPT), (2008) 2620-2625.

[12] Cheikh R., Belmili H., Drid S., Menacer A., Tiar M., Fuzzy Logic Control Algorithm of Grid Connected Doubly Fed Induction Generator Driven by Vertical Axis Wind Turbine in Variable Speed, Systems and Control (ICSC), 3rd International Conference on, (2013) 439-444.

[13] Depenbrock M., Direct Self-Control (DSC) of Inverter-Fed Induction (1988) Vol. 3, No. 4, 420-429.

[14] Mohammadi J., Vaez-Zadeh S., Afsharnia S., Daryabeigi E., A Combined Vector and Direct Power Control for DFIG-Based Wind Turbines, Sustainable Energy, IEEE Trans on, (2014) 767-775.

[15] Datta R., Ranganathan V. T., Direct Power Control of Grid-Connected Wound Rotor Induction Machine without Rotor Position Sensors, IEEE Trans. Power Electron, (2001) Vol. 16, No. 3, 390-399.

[16] Xu L., Cartwright P., Direct Active and Reactive Power Control of DFIG for Wind Energy Generation, IEEE Trans. Energy Convers, (2006) Vol. 21, No.3, 750-758.

[17] Zhi D., Xu L., Direct power control of DFIG with constant switching frequency and improved transient performance, IEEE Trans. Energy Convers, (2007)Vol. 22, No.1, 110-118.

[18] Alegria I. de, Andreu J., Ibanez P., Villate J. L., Gabiola I., Novel Power Error Vector Control for Wind Turbine with Doubly Fed Induction Generator, in Proc. 30th Annu. Conference IEEE Industrial Electronics Society, (IECON), (2004) Vol. 2, 1218-1223.

[19] Xiao-Ming G., Dan S., Ben-Teng H., Ling-Ling H., Direct Power Control for Wind-Wurbine Driven Doubly-Fed Induction Generator with Constant Switch Frequency, in Proc. International Conference Electrical Machines and Systems, (2007) 253-258.

[20] Fuentes E., Kalise D., Rodriguez J., Kennel R.M., Cascade-Free Predictive Speed Control for Electrical Drives, IEEE Trans. Industrial Electronics, (2014) 2176-2184.

[21] Rameshkumar K., Sakthivel A., Vijayakumar P., Senthilkumar A., Performance Analysis of Model Predictive Control for Voltage Source Inverter, Green Computing Communication and Electrical Engineering (ICGCCEE), International Conference on, (2014) 1-5,.

[22] Yongsoo C., Woo J.C., Kyo-Beum L., Model Predictive Control using a Three-Level Inverter for Induction Motors with Torque Ripple Reduction, Industrial Technology (ICIT), IEEE International Conference on, (2014)187-192.

[23] Yongchang Z., Haitao Y., Model Predictive Torque Control of Induction Motor Drives With Optimal Duty Cycle Control, Power Electronics, IEEE Trans on, (2014) 6593-6603.

[24] Xin-fang Z., Da-ping X., Yi-bing L., Predictive Functional Control of a Doubly Fed Induction Generator for Variable Speed Wind Turbines, in Proc. IEEE World Congress on Intelligent Control and Automation, (2004) Vol. 4, 3315-3319.

[25] Abad G., Ángel R.M., Poza J., Three-Level npc Converter-Based Predictive Direct Power Control of the Doubly Fed Induction Machine at Low Constant Switching Frequency, IEEE Trans. Ind. Electron, (2008)Vol. 55, No. 12, 4417-4429.

[26] Xiangjie L., Xiaobing K.,: Nonlinear Model Predictive Control for DFIG-Based Wind Power Generation, Automation Science and Engineering, IEEE Trans on, (2013)1-10.

[27] Camacho E.F., Bordons A.C., Model Predictive Control, Springer, (2004).
[28] Aggarwal A., Saini L.M., Singh B., Control Strategies for DFIG Based Grid Connected Wind Energy Conversion System, International Journal of Grid Distribution Computing, (2014) Vol.7, No.3, 49-60.
[29] Liuping W., Model Predictive Control System Design and Implementation Using MATLAB, Springer, (2009).
[30] Xu L., Cartwright P., Direct Active and Reactive Power Control of DFIG for Wind Energy Generation, IEEE Trans Energy Convers, (2006) Vol. 21, No. 3, 750-758.
[31] Eliasi H., Menhaj M.B., Davilu H., Robust Nonlinear Model Predictive Control for a PWR Nuclear Power Plant, Progress in Nuclear Energy, Elsevier, (2012) Vol.54, No.1, 177-185.
[32] Eliasi H., Menhaj M.B., Davilu H., Robust Nonlinear Model Predictive Control for Nuclear Power Plants in Load Following Operations with Bounded Xenon Oscillations, Nuclear Engineering and Design, Elsevier, (2011)Vol.241, No.2, 533-543.
[33] Eliasi H., Davilu H., Menhaj M.B., Adaptive Fuzzy Model Based Predictive Control of Nuclear Steam Generators, Nuclear Engineering and Design, Elsevier, (2007) Vol.237, No.6, 668-676.
[34] Javaheri Fard H., Najafi H.R., Predictive Algorithm in a Wind Turbine with Doubly Fed Induction Generator (DFIG) to Power Control Using the Rotor Current, 29 th International Power System Conference, Energy Research, (2014) 27-29 October; Tehran. Iran.
[35] Javaheri Fard H., Najafi H.R., Eliasi H., Direct Predictive Control Strategy of Active and Reactive Powers, Applied to the Converter AC / DC / AC, in a Double-Fed Induction Generator Based Wind Turbine, 12th Technologies of Power Electronic Seminar, Sharif seminar on power electronics, Sharif University of Technology, (2015) 3-4 March; Tehran. Iran.
Javaheri Fard H., Eliasi H., Najafi H.R., Direct Predictive Control Strategy of Active and Reactive Powers, Applied to the Converter AC / DC / AC, in a Double-Fed Induction Generator Based Wind Turbine, 7th Electric Power Generation Conference & Exhibition (EPGC). (2015)17-18 Feb; Bandarabas. Iran.
[37] Javaheri Fard H., Najafi H.R., Najafi J., Offering a Variety of Configurations and Model Based Predictive Controller on Photovoltaic Inverter Systems, 4 th Annual Clean Energy Conference (ACEC 2014), Kerman University, (2014)25-26 June; Kerman, Iran.

Appendix a: Overall System,
Wind energy conversion system based on DFIG

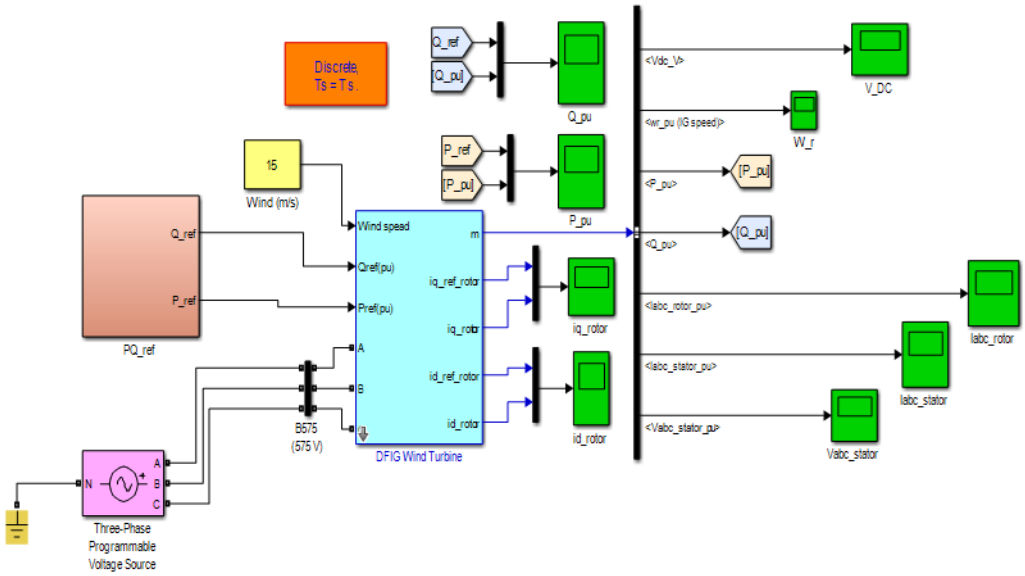

Appendix b: Controller Sub-system